

## Desalination by cooling and freezing of seawater and groundwater: thermodynamic aspect of the liquid–solid equilibrium

A. Rich<sup>a,\*</sup>, S. Mountadar<sup>a,b</sup>, F.Z. Karmil<sup>a,b</sup>, Y. Mandri<sup>c</sup>, C. Cogné<sup>c</sup>, M. Siniti<sup>a</sup>, S. Tahiri<sup>b</sup>, D. Mangin<sup>c</sup>, M. Mountadar<sup>b</sup>

<sup>a</sup>Laboratory of Water and Environment, Team of Thermodynamic, Catalysis and Surfaces, Chemistry Department, Faculty of Sciences, University Chouaib Doukkali, El Jadida (24000), Morocco, Tel. +212 666 319093; emails: rich.anouar7@gmail.com (A. Rich), smountadar@gmail.com (S. Mountadar), fatimazahrakarmil@gmail.com (F.Z. Karmil), msiniti@yahoo.fr (M. Siniti)

<sup>b</sup>Laboratory of Water and Environment, Chemistry Department, Faculty of Sciences, University Chouaib Doukkali, El Jadida (24000), Morocco, Tel. +212 523 342325; emails: tahiri.s@ucd.ac.ma (S. Tahiri), mounta\_dar@yahoo.fr (M. Mountadar)

<sup>c</sup>Laboratory of Automatic Control, Chemical and Pharmaceutical Engineering (LAGEPP), University Lyon 1, Villeurbanne 69622, France, Tel. 33 (0)4 72 43 18 51; emails: youssefmandri@gmail.com (Y. Mandri), claudia.cogne@univ-lyon1.fr (C. Cogné), denis.mangin@univ-lyon1.fr (D. Mangin)

Received 4 November 2018; Accepted 20 June 2019

---

### ABSTRACT

This work focuses on the study of the effect of water composition on the physical properties and thermodynamics of the liquid–solid equilibrium during the desalination process by cooling and freezing. The study was conducted with synthetic ionic aqueous solutions and two real systems, namely seawater from the Atlantic Ocean and groundwater from the coastal area between Ouled Ghanem and Sidi Abed (El Jadida Province, Morocco). The compositions of 73 groundwater wells were grouped statistically in three different classes. The calculation code FREZCHEM based on the thermodynamic model of Pitzer was used to estimate the following properties: activity coefficients, osmotic coefficient, ion composition, salinity, solid phases formed and their appearance temperatures at the liquid–solid equilibrium. The thermodynamic study has quantified the effect of composition and salinity on the freezing temperature, the mass of ice produced and the precipitation temperature of gypsum and mirabilite which alter the purity of ice in the desalination process.

*Keywords:* Desalination; Separation; Freezing; Cooling; Groundwater; Seawater; Liquid–solid equilibrium

---

### 1. Introduction

Access to water is one of the pressing global issues of the 21st century. Population growth in the world has accompanied an increased demand for drinking water while industrialization, irrigation of soils and rising living standards result in a further increase in the consumption of fresh water per capita. This evolution occurs mainly in coastal regions where nearly half the population of the planet lives, and this proportion will reach three-quarters by 2020 [1].

In some coastal regions in Morocco, the groundwater is not useful for drinking or even for irrigation. In general, the salinity of this groundwater varies between 1 and 14 g/L [2]. On the other hand, drinking water standards prescribed by WHO are becoming increasingly demanding (salinity of less than 1 g/L). In the coastal region between Ouled Ghanem and Sidi Abed (El Jadida province, Morocco), the mobilization of non-conventional water resources supply is a strategic long-term choice. The groundwater of this region is

---

\* Corresponding author.

characterized by the spatial evolution of dissolved salts and water composition. In general, the main factors influencing changes in groundwater composition are geological, piezometrical, chemical properties of the waters, the invasion of the coastal aquifers by marine waters and distance from the sea [3].

Desalination technologies are identified as one of the effective ways to meet this growing demand for water in coastal areas where the majority of the populations, human and industrial activities are concentrated. The most widely used techniques are distillation and reverse osmosis. Desalination by freezing has been proposed as an alternative in several recent research studies [4–8]. The complete desalination process is carried out in two steps: the first step is the water freezing allowing the production of ice deposits on a cold wall and the second step is sweating, which consists in purifying deeply the ice by effecting a fusion of the impure zones. Previous works have shown that the key operating parameters which affect the purity of ice are initial temperature, growth rate, initial solution salinity, salinity of initial ice after freezing, sweating time and sweating temperature.

Desalination by freezing could present some advantages over other techniques. Reverse osmosis uses membranes that are onerous, very sensitive to the problem of clogging and requiring pre-treatment pushed seawater. In contrary, the process by freezing method has the advantage of having a low environmental impact and has also less corrosion problems and scaling given the low levels of working temperatures. It can theoretically allow energy gain in comparison with distillation because the melting heat of ice is seven times lower than the heat of vaporization of water. Thus, the operating cost of desalination by freezing may be competitive with that of reverse osmosis and distillation. The economic estimation of the complete desalination process of seawater, based on experimental operating points, indicates that the energy consumption of a small facility could be very low using an ideal refrigerating machine operating between the sweating unit and the freezing unit [4].

In the literature, there are several studies on the experimental behaviour of the liquid–solid equilibrium of seawater at low temperature and the thermodynamic equilibrium of liquid/solid seawater at low temperature. Nelson and Thompson [9], and Gitterman [10] gave the experimental behaviour of a synthetic system consisting of the elements  $\text{Na}^+$ ,  $\text{K}^+$ ,  $\text{Mg}^{2+}$ ,  $\text{Ca}^{2+}$ ,  $\text{Cl}^-$ ,  $\text{SO}_4^{2-}$  and  $\text{H}_2\text{O}$  that can be assimilated to seawater. The two studies carried out on seawater give an identical pure ice freezing temperature of  $-1.92^\circ\text{C}$ . The authors also observe the same appearance temperature of mirabilite ( $\text{Na}_2\text{SO}_4 \cdot 10\text{H}_2\text{O}$ ) at  $-8.2^\circ\text{C}$ , hydrohalite ( $\text{NaCl} \cdot 2\text{H}_2\text{O}$ ) at  $-22.9^\circ\text{C}$ , sylvite ( $\text{KCl}$ ) and bischofite ( $\text{MgCl}_2 \cdot 12\text{H}_2\text{O}$ ) at  $-36^\circ\text{C}$ . In contrast, Gitterman [10] observed that calcium precipitated as gypsum ( $\text{CaSO}_4 \cdot 2\text{H}_2\text{O}$ ) at  $-22.2^\circ\text{C}$ , while Nelson and Thompson [9] found that it precipitated only at  $-54^\circ\text{C}$ , as antarcticite ( $\text{CaCl}_2 \cdot 6\text{H}_2\text{O}$ ). Under these conditions, the eutectic point of the mixture was obtained at  $-36^\circ\text{C}$  by Gitterman [10] and  $-54^\circ\text{C}$  by Nelson, respectively. These differences, related to calcium precipitation, are explained by the duration of the experimental protocols used. Nelson and Thompson [9] considered that the thermodynamic equilibrium was obtained quickly, while Gitterman [10] conducted his tests over 4 weeks. So Nelson did not have time to

precipitate the gypsum. As Marion and Farren [11,12] states, the results proposed by Gitterman [10] are therefore, a priori, more reliable. Precipitation of calcium carbonate  $\text{CaCO}_3$  as ikaite ( $\text{CaCO}_3 \cdot 6\text{H}_2\text{O}$ ) during seawater freezing has been reported in many publications. Its appearance temperature varies between  $-1.9^\circ\text{C}$  and  $-6.7^\circ\text{C}$  depending on the composition of the medium [13–17]. Recently, Butler et al. [18] have shown that the composition of the water also influences the temperature at which mirabilite appears. Its appearance temperature can vary between  $-1.8^\circ\text{C}$  and  $-20.6^\circ\text{C}$ .

All whose results were made at different freezing temperature and salinity conditions and were confirmed mainly by a set of theoretical calculations. Moreover, precipitation depends not only on the freezing temperature but also on the kinetic modalities, the nature of the equilibrium established between the precipitated phases and the ionic composition [19,20]. The thermodynamic study quantifies the effect of the ionic composition and salinity of seawater on the precipitated mineral phases as a function of composition at different temperatures of freezing. The theoretical sequence of fractional crystallization was developed by Jacobus Henricus van't Hoff (1900) from the determination of solubility as well as salt saturation points [21]. Pitzer calculation of liquid–solid equilibrium was based on the ion interaction model that was well developed by Marion et al. [11,12].

The present work is devoted to the study of the thermodynamic properties of liquid–solid equilibria, on the one hand, of synthetic ionic solutions and, on the other hand, of seawater and groundwater in a temperature range of  $0^\circ\text{C}$  to  $-8^\circ\text{C}$  and a salinity of up to 140 g/kg. These properties allow understanding and predicting the various interactions between the predominant elements of water samples at liquid/solid equilibrium. Knowledge of these thermodynamic properties is indeed essential to study the freezing desalination process and interpret the phenomena involved. It makes it possible to understand and predict the various interactions between the chemical elements dissolved in the liquid phase and the other solid phases and consequently to optimize the operating conditions in the freezing desalination unit. This includes interpreting and better understanding the effects of operating conditions affecting freezing (crystallization) and purification (sweating), such as the initial and final temperatures and duration of the cooling ramp applied for freezing, the temperature and duration applied for sweating.

## 2. Materials and methods

### 2.1. Sampling areas of groundwater and seawater

Fig. 1 shows the geographical location of groundwater wells considered in this study. The area is a part of the Sahel-Doukkala basin, which belongs to the Moroccan coastal Meseta. It is bounded in the West and North by the Atlantic Ocean, in the North East by the locality of Sidi Abed and by Jemaat Ouled Ghanem in the South-West. It extends over a length of 30 km and a width of 4 km with respect to the sea. The area is about 120 km<sup>2</sup>. The study area is a part of El Jadida province which is experiencing significant population growth and an intensification of socio-economic activities.

Marine water was collected from Rabat (Morocco) coast. The city is located on the Atlantic Ocean.

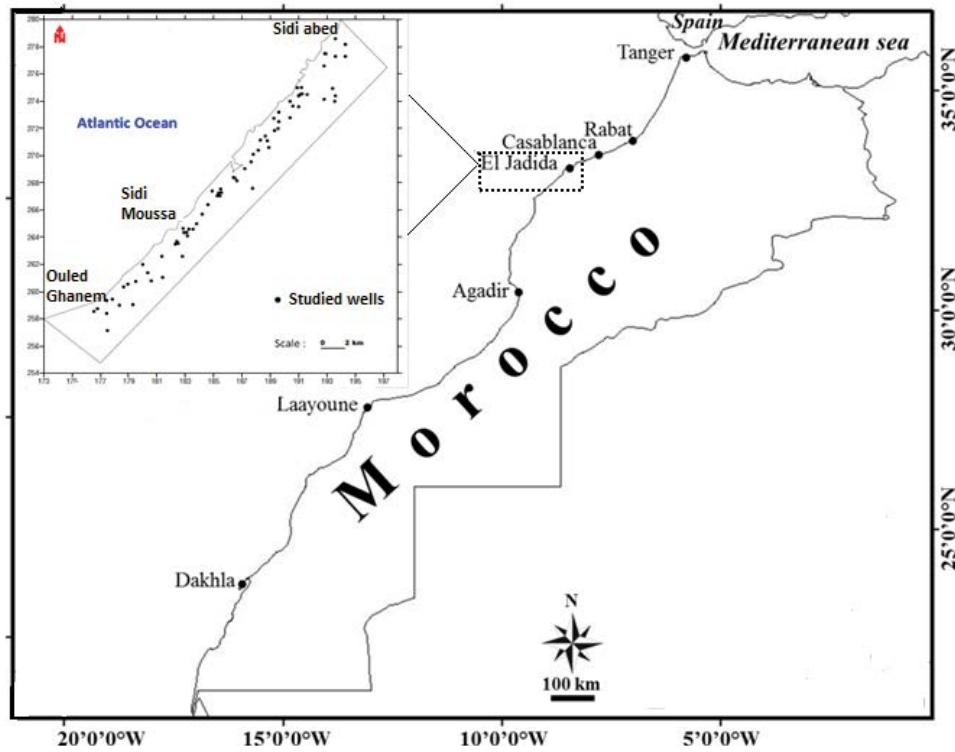


Fig. 1. Geographical location of the studied wells.

2.2. Physico-chemical characterization of groundwater and seawater

The physico-chemical characteristics of groundwater samples from 73 wells and of seawater were examined. Table 1 includes the characterization of drinking water, three wells from the three different classes of groundwater and marine water. The composition of the marine water was analyzed by ICP-AES and the compositions of the groundwater were analyzed according to the standards of AFNOR (1998) [21,23]. The groundwater in this area is generally hard, saline and does not comply with drinking and irrigation water standards. Thus, it is necessary to treat these waters to reduce their impact on the population and agricultural production.

The analysis of the 73 wells showed that groundwater can be divided into three different classes:

- *Class 1*: waters are rich in  $SO_4^{2-}$  and  $Ca^{2+}$  ions and poor in  $Na^+$  and  $Cl^-$  ions;
- *Class 2*: waters have average chemical compositions ( $Ca^{2+}$ ,  $SO_4^{2-}$ ,  $Mg^{2+}$ ,  $Na^+$  and  $Cl^-$ );
- *Class 3*: waters are rich in  $Na^+$  and  $Cl^-$  ions and poor in  $Ca^{2+}$  and  $SO_4^{2-}$  ions.

The analyses also show that the amount of  $Na^+$  and  $Cl^-$  elements represent 50%, 58%, 65% and 84.5% of the total mass of dissolved substances for class 1, class 2, class 3 and marine water, respectively. On the other hand, it is found that the salinities of the three classes of groundwater are, respectively,

Table 1  
Physico-chemical characterization of drinking water, three classes of groundwater and seawater

Parameters	Drinking water	Three classes of groundwater			Seawater
		Class 1	Class 2	Class 3	
Na <sup>+</sup> (mg/L)	<150	287.50	460.25	313.50	10,276.91–11,336.11
Cl <sup>-</sup> (mg/L)	<200	491.56	809.50	571.17	19,776.90–20,230.50
SO <sub>4</sub> <sup>2-</sup> (mg/L)	<250	504.95	590.02	242.03	2,492–3,865
Ca <sup>2+</sup> (mg/L)	<108	220.11	200.40	130.05	233.60–239.54
Mg <sup>2+</sup> (mg/L)	<50	60.06	131.26	88.12	1,277.22–1,325.12
K <sup>+</sup> (mg/L)	<12	1.95	3.919	5.87	913.89–954.52
Conductivity (mS/cm)	0.2 × 0.4	2.12	3.52	3.31	62.4
Sum of concentrations (g/L)	<1	1.56	2.19	1.35	34.97–37.95

in the order of 1.6, 2.2 and 1.4 g/L. However, the salinity of marine water is in the range of 34.97–37.95 g/L.

### 2.3. Experimental set-up and procedure

The experimental study focused on the solid–liquid equilibrium of the marine water and six synthetic solutions containing the predominant impurities of ground-water and seawater. Three synthetic solutions containing  $\text{Na}^+$ ,  $\text{Cl}^-$ ,  $\text{SO}_4^{2-}$  and  $\text{H}_2\text{O}$  were studied for the following three initial mass ratios:  $m(\text{NaCl}) = 6m(\text{Na}_2\text{SO}_4)$  (solution 1),  $m(\text{NaCl}) = m(\text{Na}_2\text{SO}_4)$  (solution 2) and  $2m(\text{NaCl}) = m(\text{Na}_2\text{SO}_4)$  (solution 3). Three synthetic solutions containing  $\text{Na}^+$ ,  $\text{Cl}^-$ ,  $\text{SO}_4^{2-}$ ,  $\text{Mg}^{2+}$  and  $\text{H}_2\text{O}$  were studied for the following three initial mass ratios:  $2.5m(\text{NaCl}) = m(\text{Na}_2\text{SO}_4) = m(\text{MgSO}_4)$  (solution 4),  $m(\text{NaCl}) = m(\text{Na}_2\text{SO}_4) = m(\text{MgSO}_4)$  (solution 5) and  $m(\text{NaCl}) = 10m(\text{Na}_2\text{SO}_4) = 10m(\text{MgSO}_4)$  (solution 6). Fig. 2 shows the experimental set-up used for studying the liquid–solid equilibria.

The assembly consists of a dual wrapped stirred vessel connected to a thermostated bath. A grid placed inside the tank keeps the ice cubes immersed in the solution. The solution of known composition is cooled in the vessel, and then stabilized at the desired temperature. A mass of about 100 g of ice cubes is then introduced into the solution. The initial concentration/temperature couple is chosen so that a fraction of the ice cubes partially melts to reach equilibrium conditions. Preliminary tests showed that the equilibrium was largely achieved after 4 h. A constant temperature plateau of 4 h was, therefore, systematically applied for each of the experimental points. The salinity of solutions in equilibrium was measured by dry extract.

### 2.4. Solid–liquid equilibrium calculation

The calculation of the liquid–solid equilibrium is based on the estimation of the solubility product  $K_s$  (Eq. (1)) related to the appearance or disappearance of a hydrated precipitate at liquid–solid equilibrium:

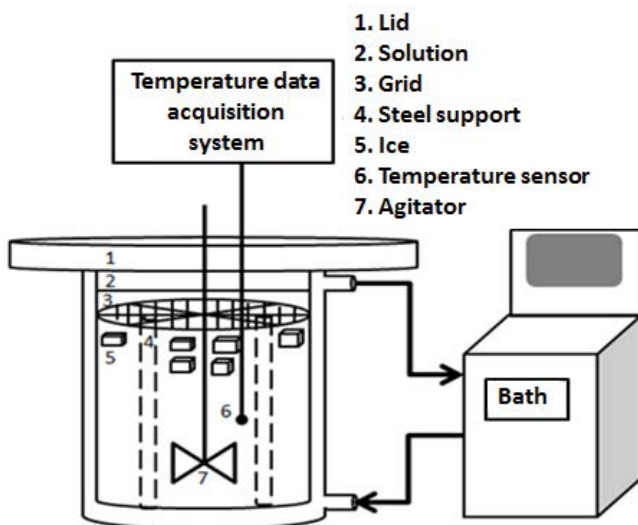


Fig. 2. Experimental set-up used for the study of the liquid–solid equilibrium.



$$K_s = \frac{(\gamma_A m_A)^{v-} (\gamma_C m_C)^{v+} (a_{\text{H}_2\text{O}})^x}{a_{A_{v-}C_{v+}, x\text{H}_2\text{O}}} \quad (1)$$

$m_A$ ,  $\gamma_A$  and  $v_-$  are, respectively, the molarity, the activity coefficient and the stoichiometric coefficient of the anion;  $m_C$ ,  $\gamma_C$  and  $v_+$  are, respectively, the molarity, the activity coefficient and the stoichiometric coefficient of the cation;  $a_{A_{v-}C_{v+}, x\text{H}_2\text{O}}$  is the activity of the precipitate equal to the unit;  $a_{\text{H}_2\text{O}}$  is the water activity, it is calculated by the following relation:

$$\ln a_{\text{H}_2\text{O}} = -\frac{1,000}{18} \phi \sum_i m_i \quad (2)$$

$\sum_i m_i$  is the sum of molarities of the ions;  $\phi$  is the osmotic coefficient.

The FREZCHEM (FREZzing CHEMistry) calculation code based on the Pitzer model [11,12,24] was used to determine the activity coefficients and the osmotic coefficient. The parameters  $P(T)$  of binary and ternary interactions of the model and the solubility products  $K_s(T)$  were expressed as a function of temperature in the following form:

$$P(T) = a_{1j} + a_{2j}T + a_{3j}T^2 + a_{4j}T^3 + \frac{a_{5j}}{T} + a_{6j} \ln T \quad (3)$$

$$K_s(T) = a'_{1j} + a'_{2j}T + a'_{3j}T^2 + a'_{4j}T^3 + \frac{a'_{5j}}{T} + a'_{6j} \ln T \quad (4)$$

where  $a_{ij}$  are coefficients specific to each interaction parameter or solubility product.

Tables 2 and 3 show the compositions entered in the calculation code FREZCHEM for the six synthetic solutions, the three classes of groundwater and three compositions of marine waters. The maximum and minimum values for the composition of groundwater and marine water cannot be entered directly into the calculation code FREZCHEM because the electroneutrality of the solution is not verified. Three compositions were chosen for which the molarities of  $\text{Na}^+$ ,  $\text{Cl}^-$  and  $\text{Mg}^{2+}$  correspond to the minimum, maximum and average values measured and the concentrations of  $\text{SO}_4^{2-}$ ,  $\text{Ca}^{2+}$  and  $\text{K}^+$  were slightly adjusted for seawater to satisfy electroneutrality. The concentration of  $\text{Cl}^-$  ions was also slightly adjusted for the three groundwater classes to verify electroneutrality. The other minority species present in the seawater or in the groundwater were not considered in the modelling.

## 3. Results and discussion

### 3.1. Liquid–solid equilibrium system $\text{Na}^+$ , $\text{Cl}^-$ , $\text{SO}_4^{2-}$ and $\text{H}_2\text{O}$

Fig. 3 compares the evolution of experimental salinity as a function of temperature with that calculated by the Frezchem/Pitzer model for the three global ratios studied of the system  $\text{Na}^+$ ,  $\text{Cl}^-$ ,  $\text{SO}_4^{2-}$  and  $\text{H}_2\text{O}$ . Table 4 recapitulates the appearance temperatures of solid phases and mass at

Table 2

Compositions of the various waters entered into the FREZCHEM calculation code for the study of the liquid–solid equilibrium of synthetic solutions

Composition	Solution					
	1	2	3	4	5	6
Cl <sup>-</sup> (mol/kg)	0.08555	0.08550	0.03420	0.08555	0.03422	0.01711
Na <sup>+</sup> (mol/kg)	0.09729	0.15590	0.09040	0.09259	0.06238	0.05231
SO <sub>4</sub> <sup>2-</sup> (mol/kg)	0.00587	0.03520	0.02810	0.00767	0.03069	0.03836
Mg <sup>2+</sup> (mol/kg)	–	–	–	0.00415	0.01661	0.02076
Salinity (g/kg)	5.83360	9.99683	5.99019	5.99983	6.00127	6.00135

Solution 1:  $m(\text{NaCl}) = 6m(\text{Na}_2\text{SO}_4)$ ; Solution 4:  $m(\text{NaCl}) = 10m(\text{Na}_2\text{SO}_4) = 10m(\text{MgSO}_4)$ ;  
 Solution 2:  $m(\text{NaCl}) = m(\text{Na}_2\text{SO}_4)$ ; Solution 5:  $m(\text{NaCl}) = m(\text{Na}_2\text{SO}_4) = m(\text{MgSO}_4)$ ;  
 Solution 3:  $2m(\text{NaCl}) = m(\text{Na}_2\text{SO}_4)$ ; Solution 6:  $2.5m(\text{NaCl}) = m(\text{Na}_2\text{SO}_4) = m(\text{MgSO}_4)$ .

Table 3

Compositions of the various waters entered into the FREZCHEM calculation code for the study of the liquid–solid equilibrium of groundwater and marine water

Solutions	Groundwater				Marine water	
	7 (Class 1)	8 (Class 2)	9 (Class 3)	10 (Minimal)	11 (Average)	12 (Maximal)
Cl <sup>-</sup> (mol/kg)	0.00745	0.01635	0.01744	0.55710	0.56348	0.56985
Na <sup>+</sup> (mol/kg)	0.01250	0.02001	0.01363	0.44682	0.46984	0.49286
SO <sub>4</sub> <sup>2-</sup> (mol/kg)	0.01051	0.01228	0.00504	0.02045	0.02734	0.03424
Mg <sup>2+</sup> (mol/kg)	0.00247	0.00540	0.00363	0.05256	0.05356	0.05453
Ca <sup>2+</sup> (mol/kg)	0.00549	0.00500	0.00324	0.00783	0.00688	0.00597
K <sup>+</sup> (mol/kg)	0.00005	0.00010	0.00015	0.03040	0.02744	0.02447
Salinity (g/kg)	1.84411	2.55638	1.64094	34.79595	36.08479	37.37473

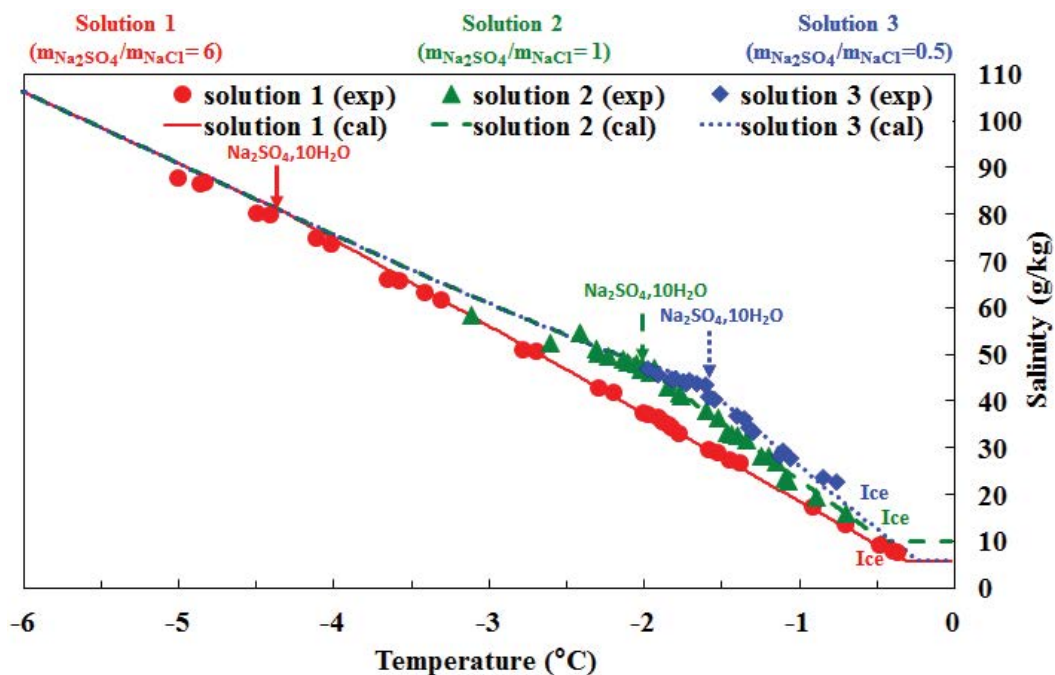


Fig. 3. Experimental and calculated salinities of the liquid–solid equilibrium for the system Na<sup>+</sup>, Cl<sup>-</sup>, SO<sub>4</sub><sup>2-</sup> and H<sub>2</sub>O.

Table 4

Appearance temperatures of solid phases and mass at liquid–solid equilibrium for the system  $\text{Na}^+$ ,  $\text{Cl}^-$ ,  $\text{SO}_4^{2-}$  and  $\text{H}_2\text{O}$ 

Solution	Solution 1		Solution 2		Solution 3	
Initial mass ratios	$m(\text{NaCl}) = 6 m(\text{Na}_2\text{SO}_4)$		$m(\text{NaCl}) = m(\text{Na}_2\text{SO}_4)$		$2m(\text{NaCl}) = m(\text{Na}_2\text{SO}_4)$	
Temperature ( $^\circ\text{C}$ )	-0.29	-4.40	-0.42	-2.05	-0.22	-1.65
Ice mass (g)	5.05	928.56	4.84	795.08	29.65	867.99
$\text{Na}_2\text{SO}_4 \cdot 10\text{H}_2\text{O}$ mass (g)	0	0.08	0	0.07	0	0.03

liquid–solid equilibrium between  $0^\circ\text{C}$  and  $-6^\circ\text{C}$  for the system  $\text{Na}^+$ ,  $\text{Cl}^-$ ,  $\text{SO}_4^{2-}$  and  $\text{H}_2\text{O}$ . The model predicts the presence of ice below  $-0.29^\circ\text{C}$  for solution 1 [ $m(\text{NaCl}) = 6 m(\text{Na}_2\text{SO}_4)$ ],  $-0.42^\circ\text{C}$  for solution 2 [ $m(\text{NaCl}) = m(\text{Na}_2\text{SO}_4)$ ] and  $-0.22^\circ\text{C}$  for solution 3 [ $2m(\text{NaCl}) = m(\text{Na}_2\text{SO}_4)$ ]. Fig. 3 shows that, at high temperatures, ice is the only solid phase present. The discontinuity, marked by an arrow on each of the curves, corresponds to the temperature at which the crystals of mirabilite ( $\text{Na}_2\text{SO}_4 \cdot 10\text{H}_2\text{O}$ ) appear ( $T = -1.65^\circ\text{C}$  for the ratio  $2m(\text{NaCl}) = m(\text{Na}_2\text{SO}_4)$ ,  $T = -2.05^\circ\text{C}$  for the ratio  $m(\text{NaCl}) = m(\text{Na}_2\text{SO}_4)$  and  $T = -4.4^\circ\text{C}$  for the ratio  $m(\text{NaCl}) = 6m(\text{Na}_2\text{SO}_4)$ ). The mass of ice formed between the freezing temperature and the precipitation temperature of  $\text{Na}_2\text{SO}_4 \cdot 10\text{H}_2\text{O}$  is approximately 867.99 g for the ratio  $2m(\text{NaCl}) = m(\text{Na}_2\text{SO}_4)$ , about 795.08 g for the ratio  $m(\text{NaCl}) = m(\text{Na}_2\text{SO}_4)$  and about 928.56 g for the ratio  $m(\text{NaCl}) = 6m(\text{Na}_2\text{SO}_4)$ . Beyond this last point, two solid phases coexist and the curve becomes a cotectic line. For each of the three ratios, the presence of a white solid phase in suspension with the ice cubes was observed visually in all tests carried out below this temperature. However, higher is the initial fraction of  $\text{Na}_2\text{SO}_4$ , higher is the temperature of appearance of  $\text{Na}_2\text{SO}_4 \cdot 10\text{H}_2\text{O}$  crystals. The equilibrium curves of Fig. 3 also show that the experimental salinity of the solution and the calculated one, given by

the FREZCHEM code, are in good agreement. The absolute deviation and the average relative error are, respectively, 1.03 g/kg and of 2.18%.

### 3.2. Solid–liquid equilibrium of the system $\text{Na}^+$ , $\text{Cl}^-$ , $\text{SO}_4^{2-}$ , $\text{Mg}^{2+}$ and $\text{H}_2\text{O}$

Fig. 4 gives a comparison between the evolution of the experimental salinity as a function of the temperature with that calculated by the Frezchem/Pitzer model for the three global ratios studied in the system  $\text{Na}^+$ ,  $\text{Cl}^-$ ,  $\text{SO}_4^{2-}$ ,  $\text{Mg}^{2+}$  and  $\text{H}_2\text{O}$ . Table 5 recapitulates the appearance temperatures and mass of solid phases at liquid–solid equilibrium between  $0^\circ\text{C}$  and  $-6^\circ\text{C}$  for the system  $\text{Na}^+$ ,  $\text{Cl}^-$ ,  $\text{SO}_4^{2-}$ ,  $\text{Mg}^{2+}$  and  $\text{H}_2\text{O}$ . The model predicts the presence of ice below  $-0.29^\circ\text{C}$  for solution  $m(\text{NaCl}) = 10m(\text{Na}_2\text{SO}_4) = 10m(\text{MgSO}_4)$ ,  $-0.19^\circ\text{C}$  for solution  $m(\text{NaCl}) = m(\text{Na}_2\text{SO}_4) = m(\text{MgSO}_4)$  and  $-0.19^\circ\text{C}$  for solution  $2.5m(\text{NaCl}) = m(\text{Na}_2\text{SO}_4) = m(\text{MgSO}_4)$ . Fig. 4 shows that  $\text{Na}_2\text{SO}_4 \cdot 10\text{H}_2\text{O}$  crystals are present in suspension with ice crystals below  $-2.09^\circ\text{C}$ ,  $-2.54^\circ\text{C}$  and  $-4.50^\circ\text{C}$  for the overall ratios  $2.5m(\text{NaCl}) = m(\text{Na}_2\text{SO}_4) = m(\text{MgSO}_4)$ ,  $m(\text{NaCl}) = m(\text{Na}_2\text{SO}_4) = m(\text{MgSO}_4)$  and  $m(\text{NaCl}) = 10m(\text{Na}_2\text{SO}_4) = 10m(\text{MgSO}_4)$ , respectively. The mass of ice formed between the freezing temperature and the precipitation temperature of  $\text{Na}_2\text{SO}_4 \cdot 10\text{H}_2\text{O}$  is approximately 930.26 g

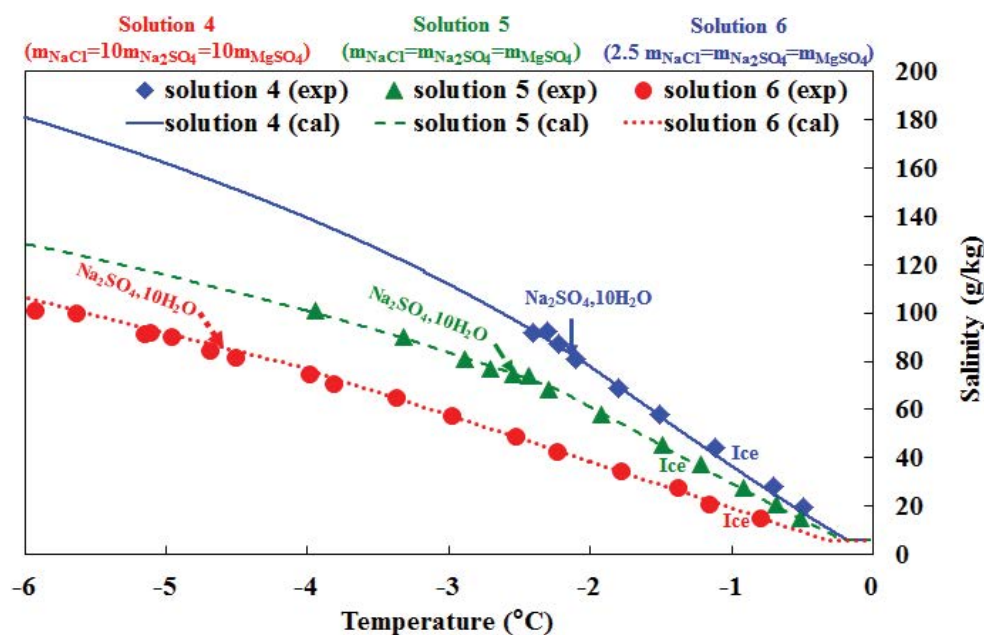


Fig. 4. Experimental and calculated salinities of the liquid–solid equilibrium for the system  $\text{Na}^+$ ,  $\text{Cl}^-$ ,  $\text{SO}_4^{2-}$ ,  $\text{Mg}^{2+}$  and  $\text{H}_2\text{O}$ .

Table 5

Appearance temperatures and mass of solid phases at liquid–solid equilibrium for the system  $\text{Na}^+$ ,  $\text{Cl}^-$ ,  $\text{Mg}^{2+}$ ,  $\text{SO}_4^{2-}$  and  $\text{H}_2\text{O}$ .

Solution	Solution 4		Solution 5		Solution 6	
Temperature (°C)	-0.29	-4.50	-0.19	-2.54	-0.19	-2.09
Ice mass (g)	7.72	930.26	11.35	929.95	3.68	929.77
$\text{Na}_2\text{SO}_4 \cdot 10\text{H}_2\text{O}$ mass (g)	0	0.45	0	2.16	0	1.00

Solution 4:  $m(\text{NaCl}) = 10m(\text{Na}_2\text{SO}_4) = 10m(\text{MgSO}_4)$ ;

Solution 5:  $m(\text{NaCl}) = m(\text{Na}_2\text{SO}_4) = m(\text{MgSO}_4)$ ;

Solution 6:  $2.5m(\text{NaCl}) = m(\text{Na}_2\text{SO}_4) = m(\text{MgSO}_4)$ .

for the ratio  $m(\text{NaCl}) = 10m(\text{Na}_2\text{SO}_4) = 10m(\text{MgSO}_4)$ , about 929.95 g for the ratio  $m(\text{NaCl}) = m(\text{Na}_2\text{SO}_4) = m(\text{MgSO}_4)$  and about 929.77 g for the ratio  $2.5m(\text{NaCl}) = 6m(\text{Na}_2\text{SO}_4) = m(\text{MgSO}_4)$ . Visual observations revealed the presence of a white solid phase in suspension with ice cubes below these temperatures. Contrary to what is observed in Fig. 3, the cotectic lines, which correspond to the equilibrium between ice, mirabilite and the solution, do not meet at low temperature in Fig. 4. Indeed, the solution composition remains different from one line to the other since the ratios  $\text{Mg}^{2+}/\text{Na}^+$  or  $\text{SO}_4^{2-}/\text{Na}^+$  are different. Besides, Fig. 4 shows that the FREZCHEM code predicts accurately the equilibrium: the difference between experimental and calculated salinities

is small: the average absolute error and the mean relative error on the salinity being, respectively, 1.3 g/kg and 2.42%.

### 3.3. Liquid–solid equilibrium of seawater

The liquid–solid equilibrium was also studied for the seawater, for which the compositions are given in Table 1 (seawater from Rabat) and Table 3 (simplified marine waters used in the model). Table 6 recapitulates the appearance temperatures and mass of solid phases at liquid–solid equilibrium between 0°C and -8°C for the three compositions of marine water. Fig. 5 shows the evolution of the experimental and calculated salinities of the solution at the equilibrium

Table 6

Appearance temperatures and mass of solid phases at liquid–solid equilibrium for the three marine waters seawater

Solution	10 (Minimum composition)		11 (Average composition)		12 (Maximum composition)	
Temperature (°C)	-1.84	-7.55	-1.89	-6.49	-1.93	-5.77
Ice mass (g)	4.30	734.81	4.84	689.62	0.42	646.89
$\text{Na}_2\text{SO}_4 \cdot 10\text{H}_2\text{O}$ mass (g)	0	0.02	0	0.02	0	0.03

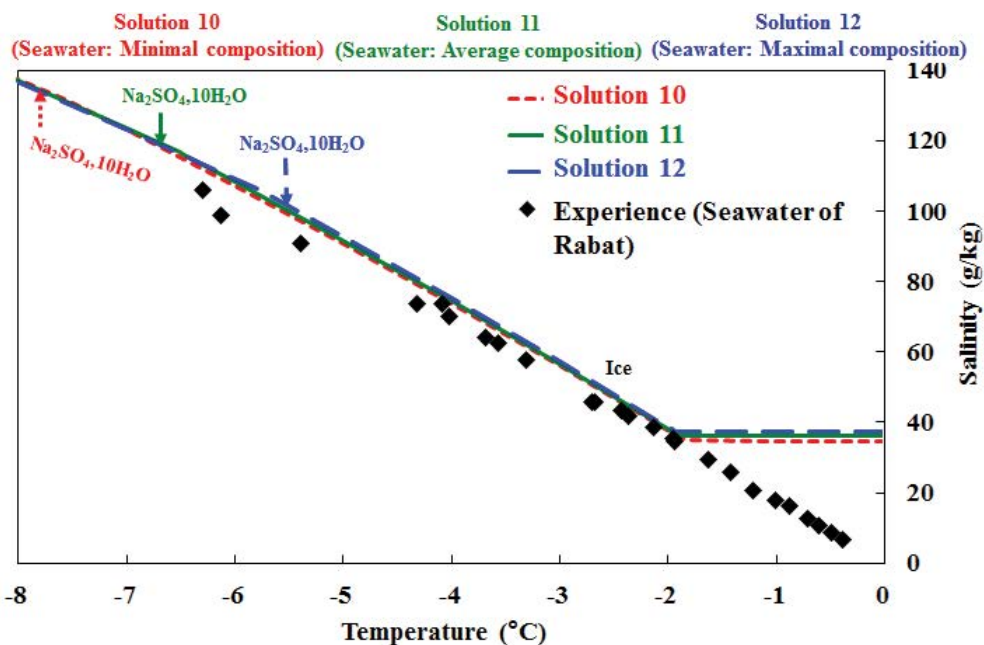


Fig. 5. Experimental and calculated salinities of the liquid–solid equilibrium for seawater.

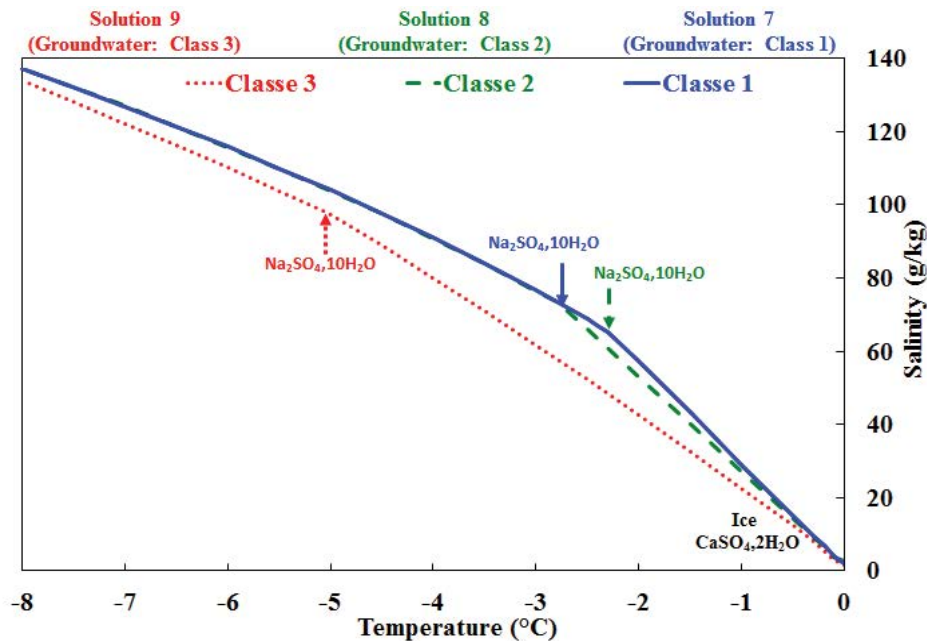


Fig. 6. Calculated salinities of the liquid–solid equilibrium for the three classes of groundwater.

Table 7

Appearance temperatures and mass of solid phases at liquid–solid equilibrium for the three groundwater classes

Solutions	Solution 7 (Class 1)		Solution 8 (Class 2)		Solution 9 (Class 3)			
Temperature (°C)	-0.1	-2.3	-0.1	-0.2	-2.8	-0.1	-0.3	-5.1
Ice mass (g)	590.70	982.31	322.21	624.35	972.93	333.69	797.04	986.66
CaSO <sub>4</sub> ·2H <sub>2</sub> O mass (g)	0.14	0.91	0	0.1	0.81	0	0.01	0.52
Na <sub>2</sub> SO <sub>4</sub> ·10H <sub>2</sub> O mass (g)	0	0.08	0	0	0.01	0	0	0.02

with the different solid phases. Let us note that experiments were also conducted with dilute seawater solutions while the calculations were only done by starting with the three marine waters (solutions 10–12). As it can be seen in Fig. 5, the agreement between the calculated salinities and the measured salinities predicted by the Frezchem/Pitzer model is good at high temperatures. The model predicts the presence of ice below  $-1.93^{\circ}\text{C}$  for the maximum composition (solution 12),  $-1.89^{\circ}\text{C}$  for the average composition (solution 11) and  $-1.84^{\circ}\text{C}$  for the minimum composition (solution 10). If the average composition of seawater is extended on the experimental salinity curve, ice appears at about  $-1.94^{\circ}\text{C}$ . The agreement between the model and the experimental measurements becomes less good below  $-4^{\circ}\text{C}$ . This difference may be related to the minority species, which are present in the seawater, but not considered in the modelling. Indeed, the more the salinity increases, the more the minority species of the real seawater are concentrated and can influence the liquid–solid equilibrium. The model predicts the appearance of  $\text{Na}_2\text{SO}_4 \cdot 10\text{H}_2\text{O}$  crystals below  $-5.77^{\circ}\text{C}$  for the maximum composition (solution 12),  $-6.49^{\circ}\text{C}$  for the average composition (solution 11) and  $-7.55^{\circ}\text{C}$  for the minimum composition (solution 10). The mass of ice formed between the freezing temperature and the precipitation temperature of  $\text{Na}_2\text{SO}_4 \cdot 10\text{H}_2\text{O}$  is approximately 734.81 g

for the minimum composition (solution 10), 689.62 g for the average composition (solution 11) and 646.89 g for the minimum composition (solution 10). The presence of this second solid phase was observed experimentally, for equilibria conducted at  $-6.11^{\circ}\text{C}$  and  $-6.29^{\circ}\text{C}$ .

#### 3.4. Liquid–solid equilibrium of groundwater

The calculation of the liquid–solid equilibrium was also estimated for the three groundwater classes. The compositions used in the calculations are given in Table 3. Fig. 6 shows the evolution of the calculated salinity of the liquid–solid equilibrium for the three groundwater classes. Table 7 recapitulates the appearance temperatures and mass of solid phases in liquid–solid equilibrium between  $0^{\circ}\text{C}$  and  $-8^{\circ}\text{C}$  for the three classes of groundwater. The model predicts the presence of ice below  $-0.1^{\circ}\text{C}$  for the three classes of groundwater and the appearance of the second solid phase, gypsum ( $\text{CaSO}_4 \cdot 2\text{H}_2\text{O}$ ), below  $-0.1^{\circ}\text{C}$  for the composition of class 1,  $-0.2^{\circ}\text{C}$  for the composition of class 2 and  $-0.3^{\circ}\text{C}$  for the composition of class 3. The presence of the third solid phase, mirabilite ( $\text{Na}_2\text{SO}_4 \cdot 10\text{H}_2\text{O}$ ), appears below  $-2.3^{\circ}\text{C}$ ,  $-2.8^{\circ}\text{C}$  and  $-5.1^{\circ}\text{C}$ , respectively, for compositions of classes 1, 2 and 3. The mass of ice formed between the freezing temperature and the precipitation temperature of  $\text{Na}_2\text{SO}_4 \cdot 10\text{H}_2\text{O}$  is

approximately 982.31 g for the first class (solution 7), 972.93 g for the second class (solution 8) and 986.66 g for the third class (solution 9). From the results obtained by the FREZCHEM calculation code, the separation of pure water for the three classes is not the same. Indeed, the composition of water in class 1 (rich in  $\text{SO}_4^{2-}$  and  $\text{Ca}^{2+}$  and low in  $\text{Na}^+$  and  $\text{Cl}^-$  ions) does not allow separation of pure water from  $-0.1^\circ\text{C}$ , while the composition of water in class 2 (average chemical compositions in  $\text{Ca}^{2+}$ ,  $\text{SO}_4^{2-}$ ,  $\text{Mg}^{2+}$ ,  $\text{Na}^+$  and  $\text{Cl}^-$ ) allows the separation of pure water in the form of ice at  $-0.2^\circ\text{C}$ . However, the composition of water in class 3 (rich in  $\text{Na}^+$  and  $\text{Cl}^-$  and low in  $\text{SO}_4^{2-}$  and  $\text{Ca}^{2+}$  ions) allows the separation of pure water in the form of ice for temperatures between  $-0.1^\circ\text{C}$  and  $-0.3^\circ\text{C}$ . It can thus be seen that in order to increase the separation of pure water during the groundwater desalination process by freezing, it is necessary to reduce the concentrations of calcium and sulphate ions.

#### 4. Conclusion

The thermodynamic study of different systems was done to quantify the effect of chemical composition and salinity of the water on the freezing temperature and the precipitation temperatures of gypsum ( $\text{CaSO}_4 \cdot 2\text{H}_2\text{O}$ ) and mirabilite ( $\text{Na}_2\text{SO}_4 \cdot 10\text{H}_2\text{O}$ ). The equilibriums of the synthetic systems studied were well described by the FREZCHEM calculation code, derived from the Pitzer model. The equilibrium of seawater is still well described at high temperatures, considering the majority elements of seawater. The precipitation of  $\text{Na}_2\text{SO}_4 \cdot 10\text{H}_2\text{O}$ , which would alter the purity of the ice in the desalination process, was found to intervene only below about  $-6^\circ\text{C}$ . For the three classes of groundwater, the freezing temperature is in the order of  $-0.1^\circ\text{C}$ . The precipitation of  $\text{CaSO}_4 \cdot 2\text{H}_2\text{O}$ , which would alter the purity of the ice, occurs below  $-0.1^\circ\text{C}$ ,  $-0.2^\circ\text{C}$  and  $-0.3^\circ\text{C}$ , respectively, for class 1 (rich in  $\text{SO}_4^{2-}$  and  $\text{Ca}^{2+}$ ), for class 2 (average chemical compositions in  $\text{Ca}^{2+}$ ,  $\text{SO}_4^{2-}$ ,  $\text{Mg}^{2+}$ ,  $\text{Na}^+$  and  $\text{Cl}^-$ ) and for class 3 (rich in  $\text{Na}^+$  and  $\text{Cl}^-$ ). The mirabilite ( $\text{Na}_2\text{SO}_4 \cdot 10\text{H}_2\text{O}$ ) precipitates below  $-2.3^\circ\text{C}$ ,  $-2.8^\circ\text{C}$  and  $-5.1^\circ\text{C}$ , respectively, for classes 1, 2 and 3. The separation of pure water was generally favoured by the reduction of calcium and sulphate ions and the increasing concentrations of sodium ions and chlorides. Also, the quantity of water separated was limited by the calcium and sulphate concentration in relationship with gypsum and mirabilite precipitation at low temperature. However, for more water recuperation in quality and quantity for different sea composition it was necessary to reduce the concentration of calcium and sulphate. The calculation code FREZCHEM can, therefore, be used for the study of the desalination process by cooling and freezing for the production of drinking water and the separation of solid phases.

#### References

- [1] National Research Council, Desalination: A National Perspective, The National Academies Press, Washington, DC, 2008.
- [2] N. El Harrak, F. Elazhar, S. Belhamidi, M. Elazhar, J. Touir, A. Elmidaoui, Performances comparison of two membranes processes: nanofiltration and reverse osmosis in brackish water desalination, *J. Mater. Environ. Sci.*, 6 (2015) 383–390.
- [3] K. Kaid Rassou, Etude des interactions entre les eaux souterraines et les eaux de surface dans le bassin cotier d'Oualidia, Doctoral Thesis, Université Cadi Ayyad, Faculty of Sciences Semailia, Marrakech, Morocco, 2009.
- [4] A. Rich, Y. Mandri, N. Bendaoud, D. Mangin, S. Abderafi, C. Bebon, N. Semlali, J.P. Klein, T. Bounahmidi, A. Bouhaouss, S. Veessler, Freezing desalination of sea water in a static layer crystallizer, *Desal. Wat. Treat.*, 13 (2010) 120–127.
- [5] A. Rich, Y. Mandri, D. Mangin, A. Rivoire, S. Abderafi, C. Bebon, N. Semlali, J.P. Klein, T. Bounahmidi, A. Bouhaouss, S. Veessler, Sea water desalination by dynamic layer melt crystallization: parametric study of the freezing and sweating steps, *J. Cryst. Growth*, 342 (2012) 110–116.
- [6] Y. Mandri, A. Rich, D. Mangin, C. Cogné, A. Rivoire, T. Bounahmidi, A. Bouhaouss, Dessalement de l'eau de mer par congélation sur parois froides: Etude paramétrique et dimensionnement du procédé. Presented at the "Actes du Congrès Annuel de la Société Française de Thermique", 28–31 May, 2013, Gerardmer, France.
- [7] A. Rich, Y. Mandri, D. Mangin, M. El Ganaoui, M. Siniti, J.P. Klein, T. Bounahmidi, A. Bouhaouss, S. Veessler, Study of a melt crystallization process for seawater desalination, *J. Mech. Eng. Autom.*, 5 (2015) 45–52.
- [8] A. Rich, Y. Mandri, Dessalement des eaux marines et saumâtres par congélation: Aspects thermodynamiques, cinétiques, paramétrique, thermique et énergétique, Editions universitaires européennes, 2017, 240 p.
- [9] K.H. Nelson, T.G. Thompson, Deposition of salts from sea water by frigid concentration, *J. Mar. Res.*, 13 (1954) 166–182.
- [10] K.E. Gitterman, Thermal Analysis of Sea Water, CRREL TL 287, USACRREL, Hanover, New Hampshire, 1937.
- [11] G.M. Marion, R.E. Farren, Mineral solubilities in the Na-K-Mg-Ca-Cl-SO<sub>4</sub>-H<sub>2</sub>O system: a re-evaluation of the sulfate chemistry in the Spencer-Møller-Weare model, *Geochimica et Cosmochimica Acta*, 63 (1999) 1305–1318.
- [12] G.M. Marion, R. Farren, A.J. Komrowski, Alternative pathways for seawater freezing, *Cold Regions Sci. Technol.*, 29 (1999) 259–266.
- [13] A. Assur, Composition of Sea Ice and Its Tensile Strength, in Arctic Sea Ice, Publication 598, National Academy of Sciences-National Research Council, 1960, pp. 106–138.
- [14] C. Richardson, Phase relationships in sea ice as a function of temperature, *J. Glaciol.*, 17 (1976) 507–519.
- [15] G.M. Marion, Carbonate mineral solubility at low temperatures in the Na-K-Mg-Ca-H-Cl-SO<sub>4</sub>-OH-HCO<sub>3</sub>-CO<sub>2</sub>-CO<sub>2</sub>-H<sub>2</sub>O system, *Geochim. Cosmochim. Acta*, 65 (2001) 1883–1896.
- [16] G.A. Maykut, B. Light, Refractive-index measurements in freezing sea-ice and sodium chloride brines, *Appl. Optics*, 34 (1995) 950–961.
- [17] S. Papadimitriou, H. Kennedy, G. Kattner, G.S. Dieckmann, D.N. Thomas, Experimental evidence for carbonate precipitation and CO<sub>2</sub> degassing during sea ice formation, *Geochim. Cosmochim. Acta*, 68 (2003) 1749–1761.
- [18] B.M. Butler, S. Papadimitriou, A. Santoro, H. Kennedy, Mirabilite solubility in equilibrium sea ice brines, *Geochim. Cosmochim. Acta*, 182 (2016) 40–54.
- [19] L.K. Sha, Concurrent fractional and equilibrium crystallisation, *Geochim. Cosmochim. Acta*, 86 (2012) 52–75.
- [20] B.M. Butler, H. Kennedy, An investigation of mineral dynamics in frozen seawater brines by direct measurement with synchrotron X-ray powder diffraction, *J. Geophys. Res. Oceans*, 120 (2015) 5686–5697.
- [21] M. Babel, B.C. Schreiber, Geochemistry of Evaporites and Evolution of Seawater, *Treatise on Geochemistry*, 2014, pp. 483–560.
- [22] A. Hayani, Mise en évidence des facteurs de salure des eaux souterraines de la zone côtière comprise entre Sidi Abed et Ouled Ghanem (Province d'El Jadida-Maroc) et possibilités de leur adoucissement sur la Duolite 206 A, Doctoral Thesis, University Chouaib Doukkali, Faculty of Sciences, El Jadida, Morocco, 2014.
- [23] AFNOR, Recueil des normes Françaises: Qualité de l'eau, 3e éd./Collection of French Standards: Water quality, 3rd ed., 1999.
- [24] G.M. Marion, J.S. Kargel, Cold Aqueous Planetary Geochemistry with FREZCHEM: From Modeling to the Search for Life at the Limits, Springer-Verlag, Berlin Heidelberg, 2008.